ADVANCES IN ATMOSPHERIC SCIENCES, VOL. 32, AUGUST 2015, 1038–1048

Sensitivity of the Warm Core of Tropical Cyclones to Solar Radiation

GE Xuyang*[1], MA Yue[1], ZHOU Shunwu[1], and Tim LI[2]

[1]*Key Laboratory of Meteorological Disaster, Collaborative Innovation Center on Forecast and Evaluation of Meteorological Disasters, Nanjing University of Information Science and Technology, Nanjing* 210044

[2]*International Pacific Research Center, University of Hawaii, Hawaii* 96822, *USA*

(Received 18 September 2014; revised 5 December 2014; accepted 26 December 2014)

ABSTRACT

To investigate the impacts of solar radiation on tropical cyclone (TC) warm-core structure (i.e., the magnitude and height), a pair of idealized simulations are conducted by specifying different strengths of solar shortwave radiation. It is found that the TC warm core is highly sensitive to the shortwave radiative effect. For the nighttime storm, a tendency for a more intense warm core is found, with an elevated height compared to its daytime counterpart. As pointed out by previous studies, the radiative cooling during nighttime destabilizes the local and large-scale environment and thus promotes deep moist convection, which enhances the TC's intensity. Due to the different inertial stabilities, the diabatic heating in the eyewall will force different secondary circulations. For a strong TC with a deeper vertical structure, this promotes a thin upper-level inflow layer. This inflow carries the lower stratospheric air with high potential temperature and descends adiabatically in the eye, resulting in significant upper-level warming. The Sawyer–Eliassen diagnosis further confirms that the height of the maximum temperature anomaly is likely attributable to the balance among the forced secondary circulations.

Key words: tropical cyclone, warm core, structure, solar radiation

Citation: Ge, X. Y., Y. Ma, S. W. Zhou, and T. Li, 2015: Sensitivity of the warm core of tropical cyclones to solar radiation. *Adv. Atmos. Sci.*, **32**(8), 1038–1048, doi: 10.1007/s00376-014-4206-0.

1. Introduction

It is well known that the warm core is a prominent feature of tropical cyclones (TCs). For a typical cyclone, its primary circulation (tangential wind) decreases with altitude. Hence, to satisfy the thermal wind balance relationship, it is required that the temperature weakens with the radius (Willoughby, 1990). The result is the so-called TC warm core. The characteristics of the warm core (i.e., the magnitude and altitude) are closely linked to TC intensity and structure. For instance, the higher the altitude of the peak warming, the lower the surface pressure and thus the more intense the TC is. Previous studies (Hawkins and Rubsam, 1968; Hawkins and Imbembo, 1976; Emanuel, 1986; Chen and Zhang, 2013) have found that the height of the maximum warm core usually occurs in the upper levels, such as 200–300 hPa. Interestingly, Stern and Nolan (2012) examined the structure of simulated TCs, and found that the warm core generally maximized in the mid-troposphere (i.e., $z = 5$–6 km, z stands for height), which was in contrast to the widely held view that this occurs in the upper troposphere. The recent observational study by Durden (2013) revealed that the altitude of the warm core shows large variability. That is, the warm core may occur anywhere between 700 and 200 hPa, and in some cases may even have multiple centers. Hence, there is debate surrounding the characteristics of the TC warm core, which encourages us to investigate the possible processes responsible for the structure of the TC warm core.

Numerous investigators (Webster and Stephens, 1980; Tao et al., 1996; Dai, 2001; Nesbitt and Zipser, 2003) have examined the impacts of the diurnal variation of solar radiation on the tropical climate system. Possible mechanisms have been put forward regarding the roles of solar variation in modulating tropical convection. Recent numerical studies (Ge et al., 2014; Melhauser and Zhang, 2014) point out that the environmental stability and deep moist convection are substantially modulated by the diurnal variation of radiation. The radiative cooling during nighttime destabilizes the local and large-scale environment and thus promotes deep moist convection, which enhances TC intensity. However, these studies mainly focused on the early stage of TC development, and the impacts of the diurnal variation of radiation on TC warm-core structure remain less clear. In the present study, the primary purpose is to demonstrate the potential impacts of solar radiation on the structure of the TC warm core.

The remainder of the paper is organized as the follows. In section 2, the characteristics of the TC warm core (i.e., the height and intensity) are discussed. Possible physical interpretations are presented in section 3. The results of sensitiv-

* Corresponding author: GE Xuyang
Email: xuyang@nuist.edu.cn

ity tests using different model schemes are presented in section 4. And finally, a short summary and further discussion is given in section 5.

2. Preliminary results

In our previous study (Ge et al., 2014), the impacts of the diurnal cycle of radiation on TC development and size were examined. Three idealized experiments were conducted by specifying different levels of solar radiation. In the control experiment (CTL), the TC developed with a full diurnal cycle of solar radiation. In the sensitivity experiments, the solar radiation was either excluded or artificially extreme. Specifically, shortwave solar radiation was excluded in the NIGHT experiment, whereas it was strongest in the DAY experiment. Further details, including a description of the model and the design of the experiments can be found in the paper (Ge et al., 2014). In the present companion study, the primary goal is to understand the possible mechanisms accounting for the structure of the TC warm core.

The simulations showed salient differences in TC development and size, especially between NIGHT and DAY. The storm in CTL bore many similarities as that in NIGHT. To emphasize the discrepancies, the NIGHT and DAY results in particular are further compared in the present study. Figure 1 displays the evolution of the intensity (represented by the central minimum sea level pressure, MSLP) in NIGHT and DAY, respectively. The weak vortices eventually develop into stronger TCs in both experiments, although there are marked differences in terms of the intensification rate. The NIGHT (DAY) simulation exhibits a faster (slower) intensification rate. For instance, in NIGHT, the MSLP starts to fall rapidly shortly after $t = 36$ h, which is nearly 24 hours earlier than in DAY. This suggests that, under the identical initial environmental conditions, the timing of rapid intensification (RI) varies with different radiative effects. Specifically, the TC is likely to develop quicker during nighttime than daytime. The possible mechanisms involved in the influence of solar radiation on TC intensification have been discussed in previous studies (Ge et al., 2014; Melhauser and Zhang, 2014).

Figure 2 compares the azimuthally averaged radial circulations and temperature perturbations during the mature stage. In this study, the temperature averaged within a particular annulus (i.e., the radius between 600 and 700 km) is taken as the environmental value, and thus the deviation from this value reflects the characteristics of the TC warm core. Importantly, when the potential temperature is used to calculate the perturbation, the features of the warm core are qualitatively similar. Hence, the perturbation temperature is selected to represent the behavior of the warm core in the following sections. Generally, in the upper outflow layer, the warming spreads outward more radially. Obviously, there are pronounced differences in the warm-core areas between NIGHT and DAY. In NIGHT, the peak of the warm core is located at the same level as the outflow layer. However, in DAY, the height of peak warming is much lower than the outflow layer. More specifically, the height of the warm core in NIGHT is $z = 12$–14 km, which is much higher than that in the DAY storm (i.e., $z = 6$–8 km). Furthermore, the magnitude is approximately 16°C in NIGHT, which is also greater than its counterpart (12°C).

The structural difference of the warm core is dynamically consistent with the intensity changes. According to the

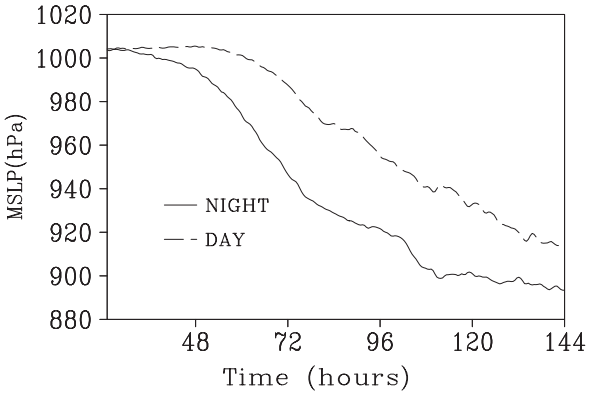

Fig. 1. Temporal evolution of tropical cyclone intensity represented by the minimum sea level pressure (MSLP, units: hPa).

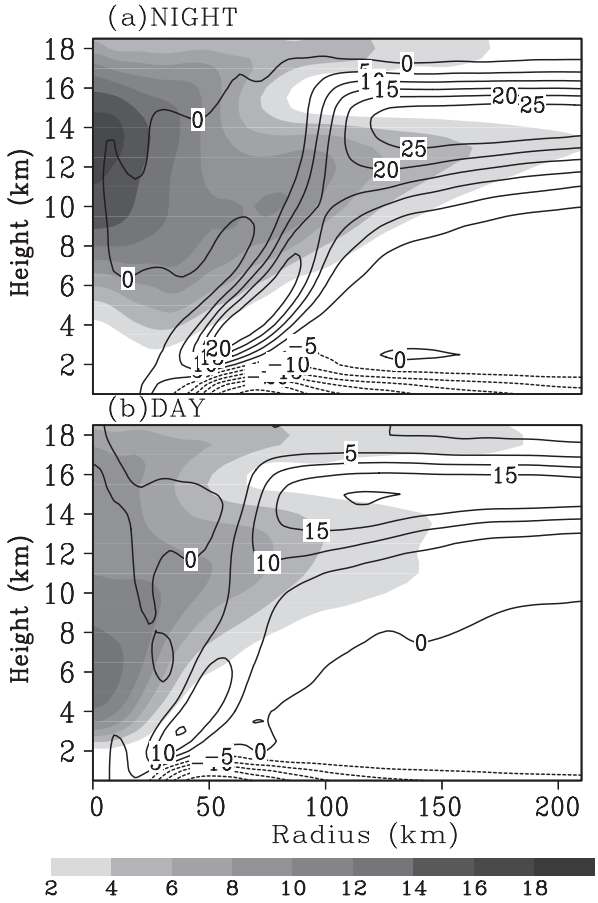

Fig. 2. The azimuthal mean of the warm core (shading; units: °C) and radial flows (contours; units: m s^{-1}) at $t = 120$ h in the (a) NIGHT and (b) DAY simulation, respectively.

hydrostatic balance relationship, the surface pressure deficit can be derived as follows:

$$\Delta P_{\rm s} = -\frac{P_{\rm s}}{T_{\rm v}(P_{\rm s})}\int_{P_{\rm s}}^{P_{\rm T}}\frac{\Delta T_{\rm v}}{P}dP\ , \qquad (1)$$

here $\Delta P_{\rm s}$ is the pressure difference between the TC center and the environment, $T_{\rm v}$ is the virtual temperature, $P_{\rm T}$ is the pressure at the top of the troposphere, and other symbols are traditional meteorological variables. It can be inferred from Eq. (1), due to the "dP/P" effect, the surface pressure will be lower if the warming anomaly is highly elevated. This agrees with the fact that the NIGHT storm has a much lower MSLP compared with the DAY storm.

Besides the differences in the magnitude and height of maximum perturbation temperature, the areal coverage of the warm core shows remarkable dissimilarities. For instance, the radial extension of the warm core in NIGHT is much wider than that in DAY, which is consistent with the fact that the former is large in size, as shown in Ge et al. (2014). For a typical TC, there is a lower (upper)-level radial inflow (outflow), and the updraft arises in the eyewall region. The maximum speed of the upper-level outflow jet exceeds 25 m s^{-1} in NIGHT, which is much faster than in DAY ($\sim$ 20 m s^{-1}). Consequently, the boundary inflow layer is slightly deeper in NIGHT, indicating a robust inward mass flux convergence, and thus helps the TC spin up. Accompanied by the strong in-up-out secondary circulation, the diabatic heating in the TC inner-core area is greatly enhanced in NIGHT.

To gain perspective on the variation of the warm core, Fig. 3 presents the time–vertical cross sections of the perturbation temperature averaged within the eye region (i.e., within a radius of 30 km). In both NIGHT and DAY, during the initially slow intensification period (prior to $t = 48$ h), there are very few temperature perturbations. Accompanied by the period of rapid intensification, pronounced warm temperature deviations are established in the middle levels ($z = 6$–8 km). For the NIGHT storm, after $t = 72$ h, a second warm core occurs in the upper troposphere (i.e., $z = 12$–16 km). During the following short period ($t = 72$–84 h), two discrete warming centers appear at $z = 6$–8 and 12–16 km, respectively. The upper-level one further intensifies and becomes the dominant one. Eventually, it exhibits a single upper warm-core structure. Note that this upper-level entity shows a slow downward displacement with time. In DAY, the peak warming center remains at an essentially constant height (about $z = 8$ km), and does not elevate very much during the whole integration.

Numerous studies (Emanuel, 1986; Holland, 1997; Braun, 2002; Knaff et al., 2004; Halverson et al., 2006; Powell et al., 2009; Chen and Zhang, 2013) have suggested that the upper-tropospheric warm core is a common characteristic of TCs. In the present study, the NIGHT storm has an upper-tropospheric warm core ($z = 14$ km), which is consistent with this widely believed viewpoint. However, in DAY, the maximum warm core occurs in the mid-troposphere ($z = 8$ km), which is similar to the findings of Stern and Nolan (2012). Given the different structure of the warm core between NIGHT and DAY, the question arises as to what causes such discrepancies. In the following section, closer examination is made to disclose the possible mechanisms involved.

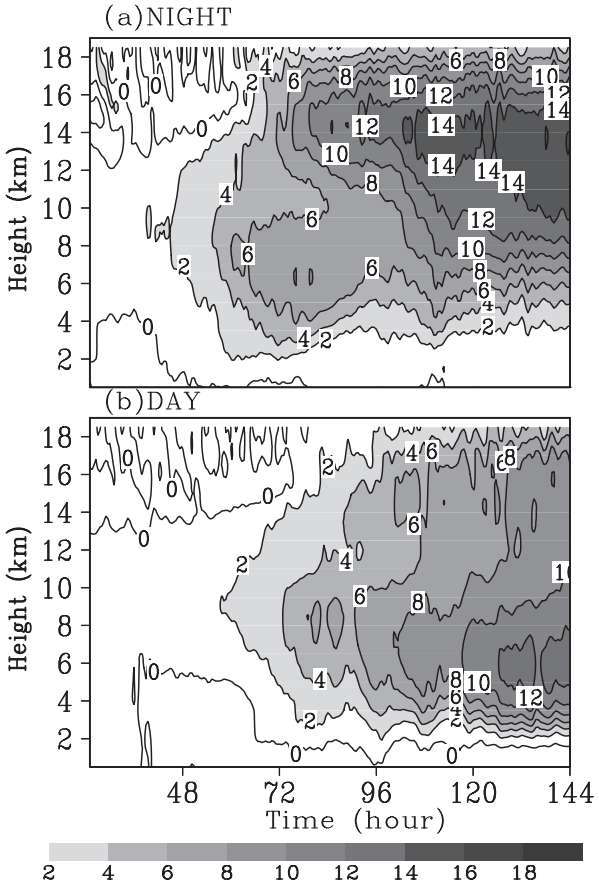

Fig. 3. Temporal evolution of the vertical profile of the warm core (units: °C) in the (a) NIGHT and (b) DAY simulation, respectively. The warm core is represented by the temperature perturbation averaged within the radius of 30 km.

3. Physical interpretations

To understand the formation of the TC warm core, the budget of potential temperature was calculated. The budget of azimuthal mean $\bar{\theta}$ is shown as the following equation:

$$\frac{\partial\bar{\theta}}{\partial t} = \mathrm{HADV} + \mathrm{VADV} + \mathrm{DHT} + \mathrm{DIFF}\ , \qquad (2)$$

where HADV $\{-\bar{u}(\partial\bar{\theta}/\partial r) - (1/r)[\partial(r\overline{u'\theta'})/\partial r]\}$ and VADV $\{-\overline{w}(\partial\bar{\theta}/\partial z) - [\partial(\overline{w'\theta'})/\partial z)]\}$ are the tendencies due to horizontal and vertical advection; DHT is diabatic heating rate; and DIFF is the tendency due to turbulence, dissipative heating, and horizontal diffusion. In the above definitions, the overbars and primes represent the azimuthal mean and the deviation from the azimuthal mean, respectively. In this study, DIFF is neglected since it is usually small in the free atmosphere (Ohno and Satoh, 2014). These tendencies were

calculated during the period between 84 h and 96 h. Figure 4 shows the radius–height cross sections of the azimuthal mean fields of the selected budget terms. It is apparent that the mean vertical advective tendency is mainly offset by the adiabatic cooling, but the residual leads to a warming around the eyewall. Of particular interest is that, in NIGHT, a significant positive tendency occurs near the height of 14 km, which is largely dominated by the horizontal advection. In contrast, there is a mid-level warming signal in DAY, but no significant tendency in the upper levels. This budget explains well the different structures of the warm core.

Numerous studies (Schubert and Hack, 1982; Hack and Schubert, 1986; Nolan et al., 2007) have suggested that the diabatic heating in the eyewall will force a secondary circulation. That is, the updraft coincides with the heating, and compensating subsidence appears on either side of the heating. These studies may explain the formation of mid-tropospheric warm cores. However, it is difficult to apply this explanation to upper-level warming via the aforementioned mechanisms, since there is little diabatic heating in the upper troposphere (i.e., above $z = 14$ km). The results here suggest that upper-level horizontal advection likely plays an important role in the formation of upper level warm cores, and thus further studies are needed.

Chen and Zhang (2013) proposed that the formation of the upper-level warm core is attributable to deep convective cells, such as vortical hot towers ("VHTs"). This motivates us to investigate the convective activity in the TC inner region. Previous studies (Ge et al., 2014; Melhauser and Zhang, 2014) have suggested that TC convective activity is highly sensitive to solar radiative effects. That is, the diurnal solar radiation can considerably modulate the pregenesis environmental conditions and thus the behavior of moist convection. In general, nighttime destabilization of the local and large-scale environment through radiative cooling may promote deep moist convection and increase the genesis potential. On the contrary, daytime solar radiation will enhance the static stability and thus suppress convection. To this end, the statistics of convective activity in the inner area are compared. Figure 5 displays the temporal evolution of the vertical distribution of grid points of deep convection. The numbers of strong updrafts within a radius of 100 km at each level are calculated. Here, vertical velocity greater than 2 m s^{-1} is considered as a strong updraft. Although the threshold of 2 m s^{-1} is somewhat arbitrary, it is true that the areal percentage of updrafts greater than this value is quiet small, and the conclusion is qualitatively similar as long as the threshold is larger than 1.5 m s^{-1}. Obviously, deep convection is much stronger in NIGHT during the whole model integration. Specifically, in NIGHT, the number is generally

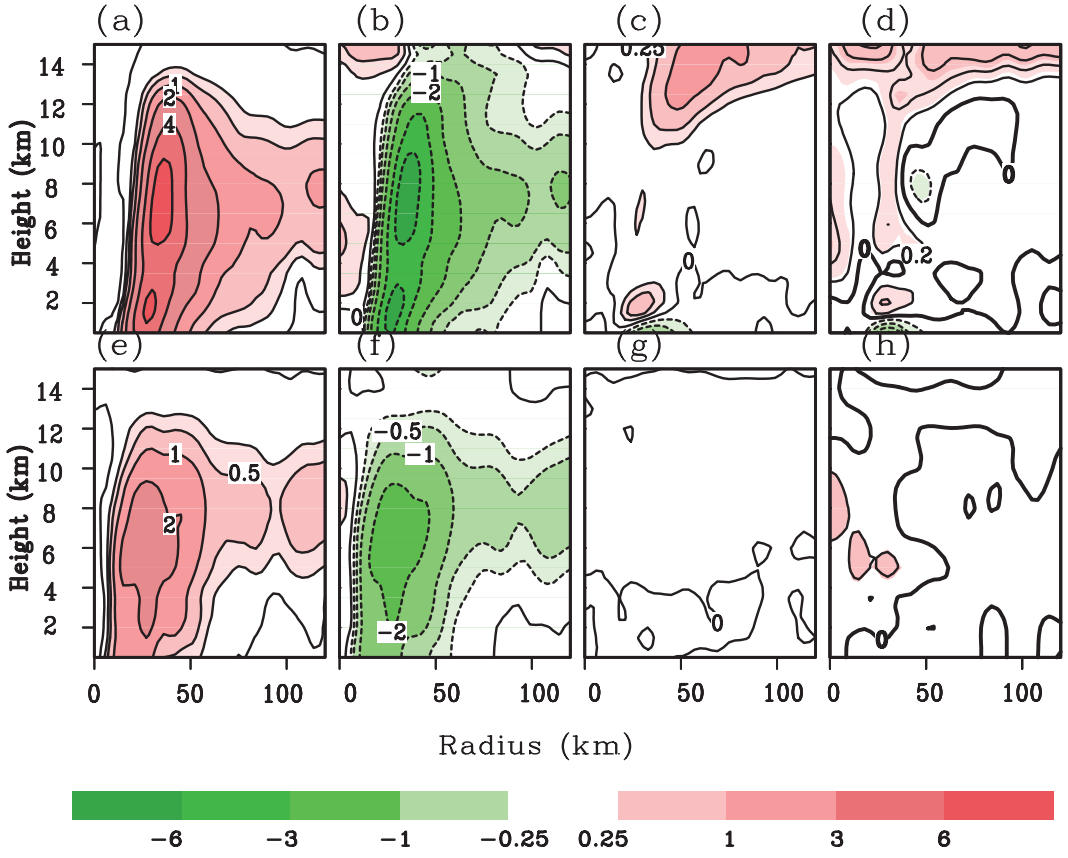

Fig. 4. Radius–height cross sections of the azimuthal mean fields of selected budget terms (units: 1×10^{-4} K s^{-1}): (a, e) diabatic heating (DHT); (b, f) vertical advection (VADV); (c, g) horizontal advection (HAVD); (d, h) the sum of the previous three terms. Panels (a–d) are for NIGHT and (e–h) for DAY.

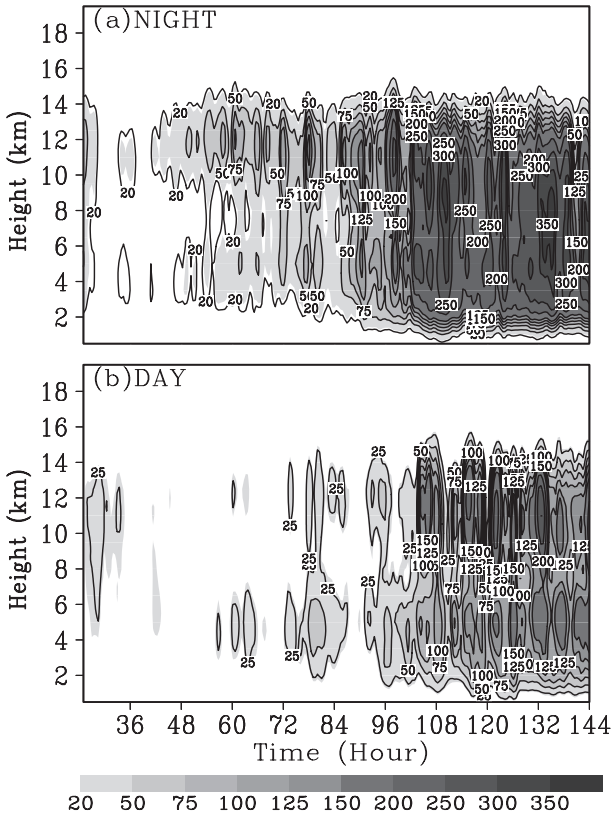

Fig. 5. Temporal evolution of the vertical distribution of the numbers of grid points with vertical velocity greater than 2 m s^{-1} in the (a) NIGHT and (b) DAY simulation.

larger than 250 after $t = 96$ h, whereas it seldom reaches 250 in DAY. This indicates that the convective activity is more active in NIGHT. Along with the increase of the updrafts, the warm core becomes more prominent.

To also gain insight into the relationship between the warm core and the inner-core convection, Figs. 6–7 compare snapshots of 200 hPa vertical motion and temperature tendency in NIGHT and DAY, respectively. Following Chen and Zhang (2013), the temperature tendency is defined as the temperature difference: $\Delta T = T_{i+1} - T_i$, where i indicates the model output at the ith time step (time interval: 15 min). Convective bursts (CBs) occur frequently in the inner core (i.e., within radius = 100 km). Generally, the CB band is conducive to cyclonic movement as the storm intensifies, and becomes more symmetric over time. Note that the areal coverage of the updraft is significant larger in NIGHT, which also coincides with pronounced positive temperature tendencies. The updraft core coincides with the maximum temperature tendency, suggesting that the CB plays an important role in the formation of the warm core. This result agrees well with Chen and Zhang (2013). Furthermore, the significant warming is likely attributable to the subsidence associated with the updrafts that penetrate into the upper troposphere (Holland et al., 1984; Heymsfield et al., 2001; Chen and Zhang, 2013). Since there is little diabatic heating within the eye, the collective effect of intense downdrafts should play an essential role. Chen and Zhang (2013) revealed that an upper inflow layer, residing just above the upper outflow channel, plays a substantial role in the establishment of the upper warm core. This inflow layer, located above the outflow layer, will effectively carry the higher potential temperature (θ) air into the TC eye, where it descends adiabatically and isentropically to induce significant warming. To test this hypothesis, Fig. 8 compares the height–radius cross section of potential temperature, vertical velocity, and radial inflow in NIGHT and DAY, separately. Notice that the surfaces of $\overline{\theta}$ in both cases are displaced downward in the inner-core region. The differences in the downward displacement suggest different locally static stabilities in the eye. Another salient feature is that a strong inflow layer is located near $z = 18$ km in NIGHT. In contrast, accompanied by a much weaker upper-level inflow, the upper-level warming is insignificant in DAY. The results suggest that the upper-level radial inflow layer likely plays an important role in upper-level warming, since the altitude of the warm core is attributable to the strength of the upper-level inflow. It is hypothesized that, while lower stratospheric air moves inward radially along the isentropic surface, the adiabatic descent may result in a warming therein. Chen and Zhang (2013) argued that this thin radial inflow layer is likely induced by the mass sink and lower pressure in the eye. To further determine the possible mechanism for this upper inflow layer, the Sawyer–Eliassen (SE) diagnosis is applied here to solve the forced problem. The SE equation in the radius-pseudoheight coordinates (Hendricks and Montgomery, 2004) can be written as

$$\frac{\partial}{\partial r}\left(\frac{A}{r}\frac{\partial\overline{\psi}}{\partial r}+\frac{B}{r}\frac{\partial\overline{\psi}}{\partial Z}\right)+\frac{\partial}{\partial Z}\left(\frac{C}{r}\frac{\partial\overline{\psi}}{\partial Z}+\frac{B}{r}\frac{\partial\overline{\psi}}{\partial r}\right) = -\frac{\partial\overline{(\xi F)}}{\partial Z}+\frac{\partial\overline{Q}}{\partial r}\,, \tag{3}$$

where the parameters are defined as $A = N^2 = (g/\theta_0)(\partial\overline{\theta}/\partial Z)$, static stability; $B = -\overline{\xi}(\partial\overline{V_t}/\partial Z)$, barocilinicity; and $C = \overline{\xi}\,\overline{\eta}$, inertial stability. Other symbols are traditional variables, and further details can be found in Hendricks and Montgomery (2004). On the right-hand side of Eq. (3), there is momentum and heating forcing, respectively. In the present study, the diabatic heating contributed by cloud microphysics is directly from the model output, and only its axisymmetric component ($\overline{Q}$) is considered.

Figure 9 displays the radial cross sections of azimuthal mean inertial stability, tangential wind, diabatic heating, and the forced mass streamfunction of secondary circulation. Figures 9a and b compare the tangential wind and the associated inertial stability in NIGHT and DAY, respectively. It is obvious that, compared with the DAY storm, the NIGHT storm has a vertically deeper structure in which the top extends to higher altitude, indicating a greater inertial stability in the inner area. Given the different inertial stabilities, the change in the local Rossby deformation radius will lead to different extensions of the response to the forcing. Schubert and Hack (1982) pointed out that, for a given heating forcing, an increase in inertial stability results in a decrease in the forced secondary circulation and thus a change in the radial distri-

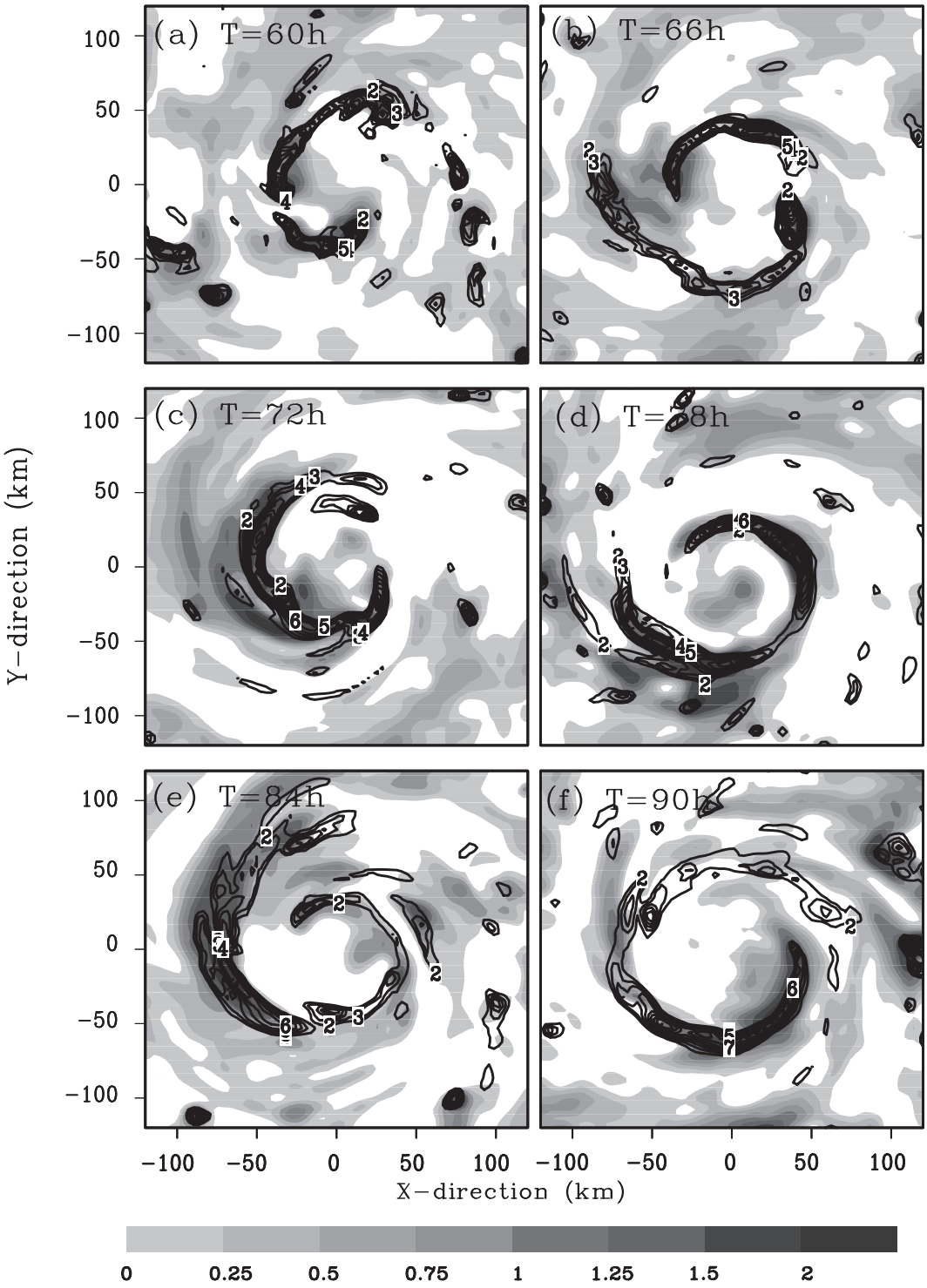

Fig. 6. Snapshots of 200 hPa vertical motion (contours; m s^{-1}) and temperature tendency (shading, units: K s^{-1}) in the NIGHT simulation at $t =$ (a) 60 h, (b) 66 h, (c) 72 h, (d) 78 h, (e) 84 h, and (f) 90 h.

bution of local temperature, with enhanced temperature tendency in the region of high inertial stability. Figures 9c and d compare the radial vertical cross section of the mass streamfunction of the secondary circulation forced by the diabatic heating. In general, the maximum mass streamfunction is located just outside the eyewall at the 10 km height, and the minimum exists inside the eyewall. This pattern is consistent with the typical in-up-out secondary circulation, with the updraft at the location of the diabatic heating. The minimum center inside the heating suggests that descending motion appears in the eye. Note the remarkable differences in the mass streamfunctions in the two cases. That is, the amplitude is much more significant in NIGHT. As such, the strong horizontal gradient of mass streamfunction results in more robust downward flow in the eye. Furthermore, the minimum streamfunction extends outward at the upper level (i.e., $z = 15$

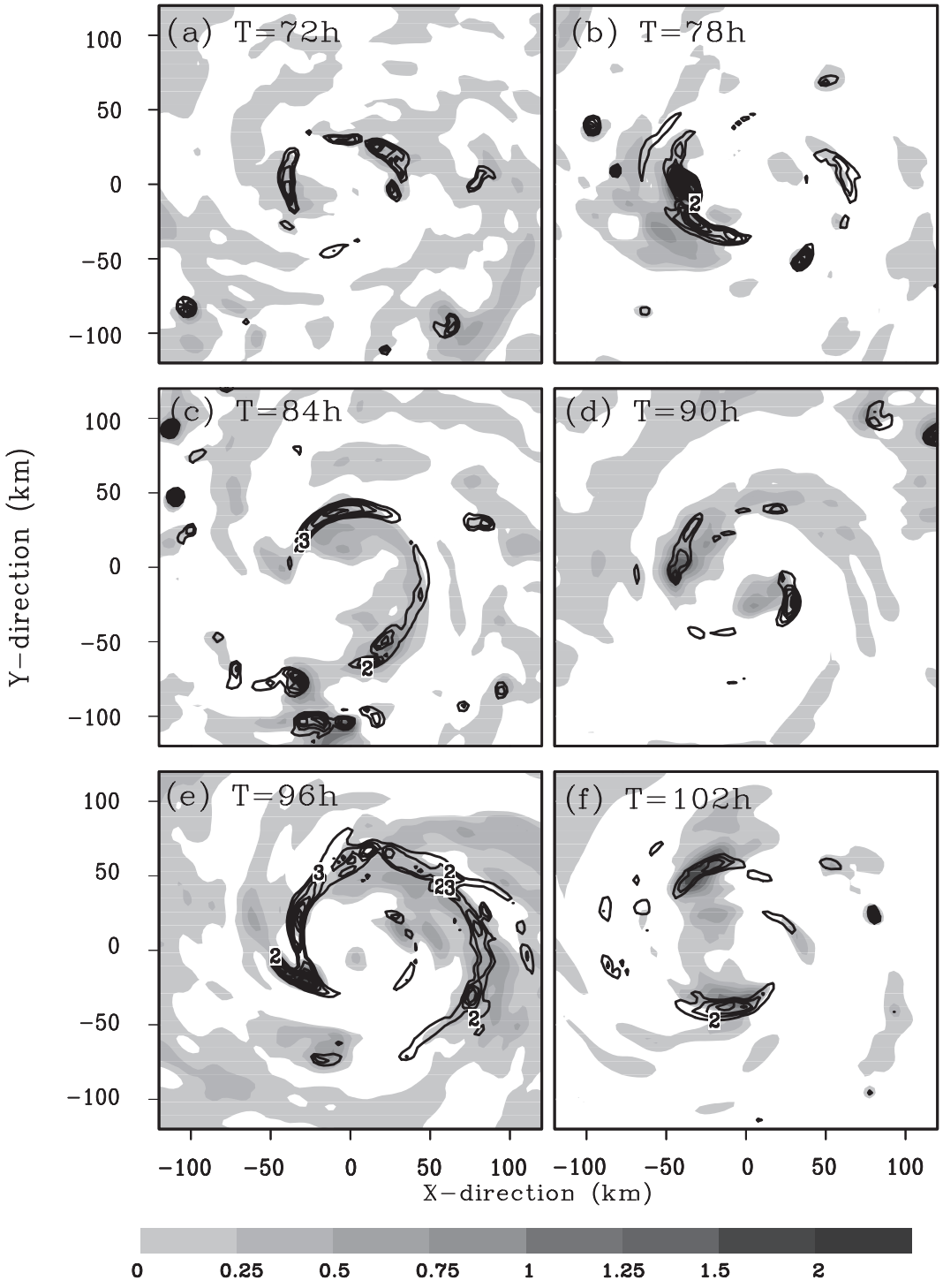

Fig. 7. The same as Fig. 6, except in the DAY simulation at t = (a) 72 h, (b) 78 h, (c) 84 h, (d) 90 h, (e) 96 h, and (f) 102 h.

km) in NIGHT. This suggests a positive vertical gradient in the inner-core area, just above 15 km. As a result, an upper-level inflow appears therein, as shown in Fig. 8. This result confirms that the upper-level inflow is forced by the TC diabatic heating. Ohno and Satoh (2014) proposed that upper-level subsidence is closely associated with TC structure. For instance, the upper-level subsidence is enhanced in the eye when the vortex is sufficiently tall to penetrate the statically stable stratosphere. It can be deduced that the height of the maximum temperature anomaly is largely attributable to the balance among forced secondary circulations. In this regard, since the NIGHT storm has both a stronger intensity and diabatic heating source, the greater inertial stability may extend the response to the heating to the upper troposphere and cause

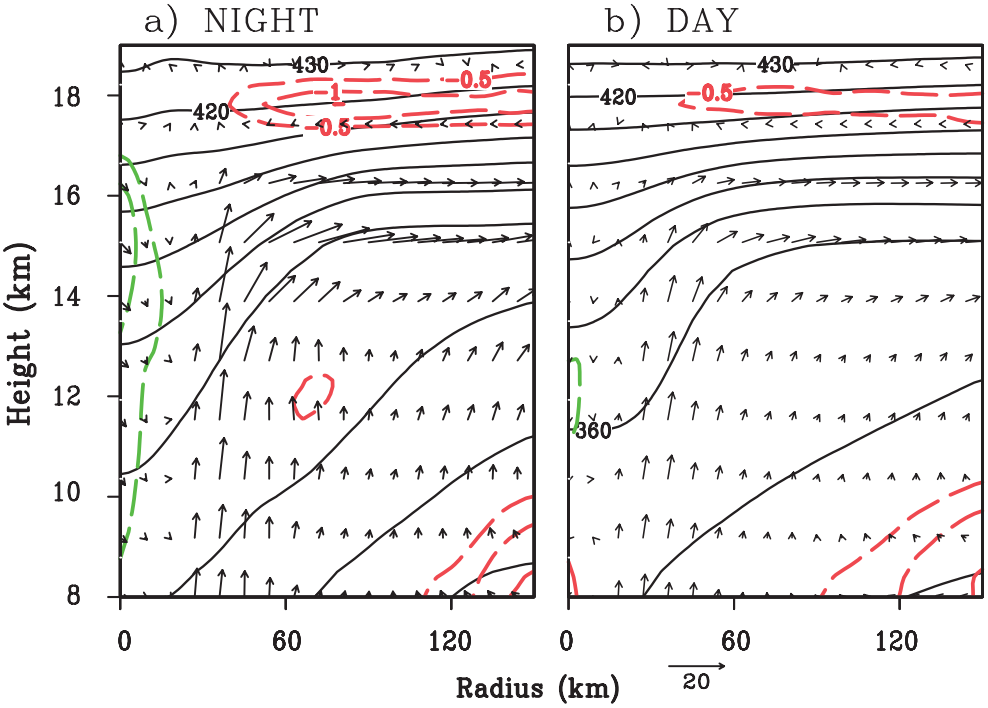

Fig. 8. Height–radius cross section of potential temperature (dark solid lines, units: K), vertical velocity (green dashed lines; negatives are plotted with intervals of 0.1 m s^{-1}), and radial inflows (red dashed lines; negatives are plotted with intervals of -0.5 m s^{-1}) at $t = 96$ h in the (a) NIGHT and (b) DAY simulation, respectively.

upper-level adiabatic warming.

4. Sensitivity to model schemes

In this section, the results of sensitivity experiments are used to examine the robustness of the above results. A series of experiments with different model schemes were conducted. The details are listed in Table 1. For the boundary layer scheme, the Yonsei University (YSU) planetary boundary layer (Hong et al., 2006) and Mellor–Yamada–Janjic (MYJ; Mellor and Yamada, 1982) schemes are commonly used for the Advanced Research Weather Research and Forecasting (WRF_ARW) model. In the control run, the YSU scheme was applied, and the MYJ scheme was examined in EXP1_D/N (D/N represents the DAY and NIGHT scenario, respectively). In EXP2_D/N, the single-moment 6-class (WSM-6) microphysics scheme (Hong and Lim, 2006) was used to compare with the Lin et al. (1983) scheme in the benchmark run. Furthermore, the Rapid Radiative Transfer Model (RRTM) longwave (Mlawer et al., 1997) parameterization scheme was applied in EXP3_D/N.

The results show that the storm intensifies more rapidly in the NIGHT scenario for all the sensitivity experiments (not shown), which agrees well with Ge et al. (2014). Note that the warm-core structures show salient differences. That is, accompanied by the more intense TC in NIGHT, an upper-level warm core emanates, whereas only a mid-tropospheric entity emerges in its counterpart. Figure 10 shows the horizontal–

Table 1. List of sensitivity experiments. See the text (section 4) for the definitions of the abbreviations.

Experiment	Microphysics	Boundary layer	Radiation
DAY/NIGHT	Lin et al. (1983)	YSU scheme	Dudhia
EXP1_D/N	Lin et al. (1983)	MYJ scheme	Dudhia
EXP2_D/N	WSM6 (Hong and Lim, 2006)	YSU scheme	Dudhia
EXP3_D/N	Lin et al. (1983)	YSU scheme	RRTM

vertical cross sections of temperature perturbations in the sensitivity experiments. It is clear that there is a distinctly higher warm core in NIGHT than in DAY, indicating that the results are robust and not sensitive to the different model configurations.

5. Conclusion

The sensitivity of TC warm-core structure to shortwave radiation was examined by conducting highly idealized experiments. It was found that solar radiation not only impacts on TC intensification, but also on the warm-core structure. In the NIGHT experiment, which excluded solar radiation, the TC favored the establishment of a significant warm core at higher altitude. Previous studies suggest that significant convective activity in the inner-core region is an important ingredient in the generation of an upper-level warm core. In the present study, Sawyer–Eliassen diagnosis further suggests

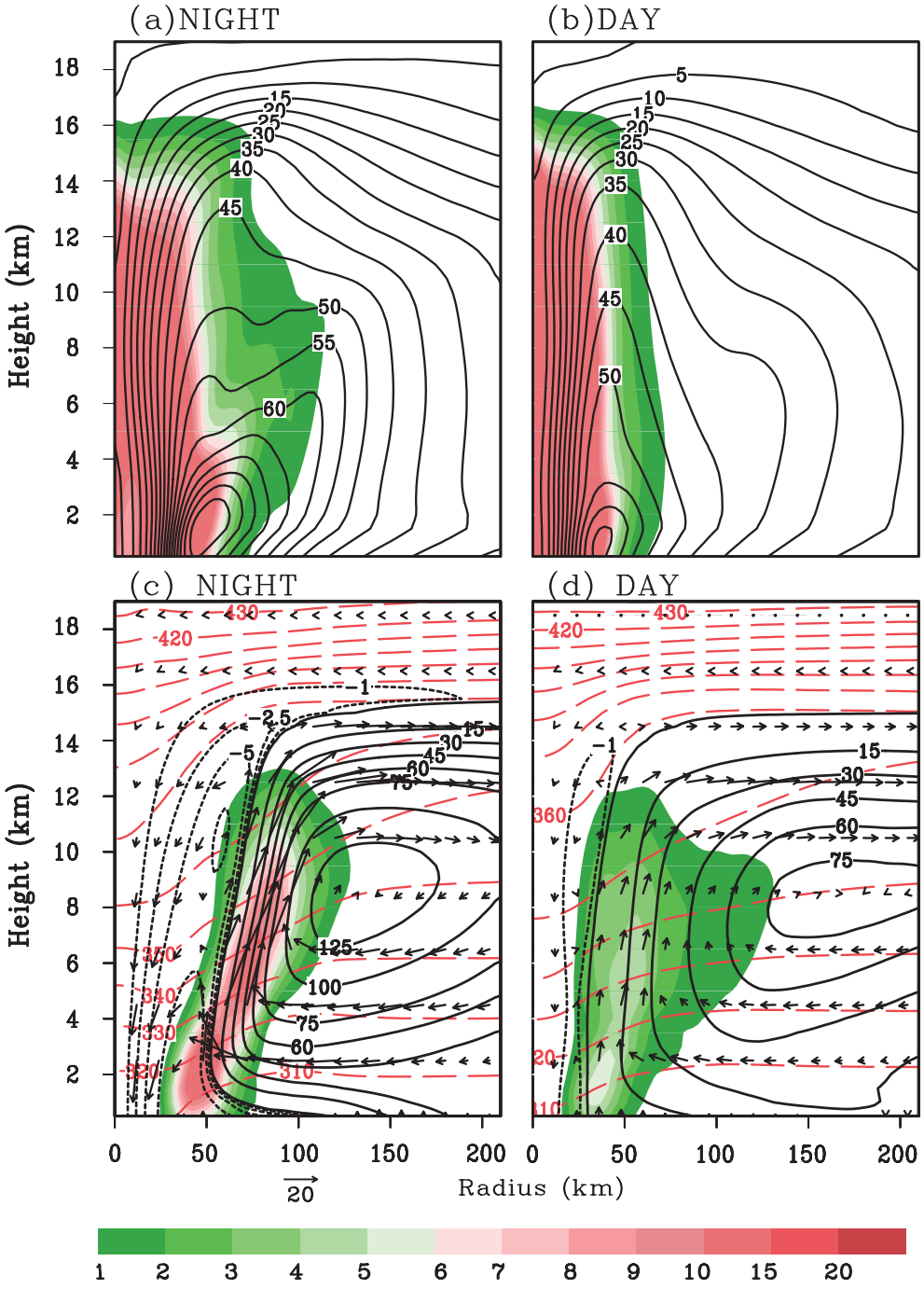

Fig. 9. Radial vertical cross sections of the tangential wind (contours, units: m s^{-1}) and inertial stability (shading) in the (a) NIGHT and (b) DAY simulation. Panels (c, d) are the same as (a, b), but for the mass streamfunction (contours) and diabatic heating forcing (shading, units: K h^{-1}) in the (c) NIGHT and (d) DAY simulation. The dashed lines in (c) and (d) are potential temperature (K). The vectors in (c, d) are the forced radial circulations.

that the height of the maximum temperature anomaly is likely attributable to the balance among forced secondary circulations. It is proposed that strong CBs lead to strong diabatic heating and thus favor a more intense TC with larger inertial stability. As a result, the forced secondary circulation promotes a thin upper-level inflow layer. This radial inflow will effectively carry the lower-stratospheric air with high potential temperature and descend adiabatically in the eye, resulting in significant upper-level warming.

Admittedly, the results are only based on highly idealized numerical simulations, since the radiation is artificially extreme. Solar radiation modulates the static stability and thus influences the convective activity, which affects TC intensity and structure. The response to the diabatic heating is sensitive to the vortex structure. With different inertial stability, the diabatic heating in the eyewall will force different

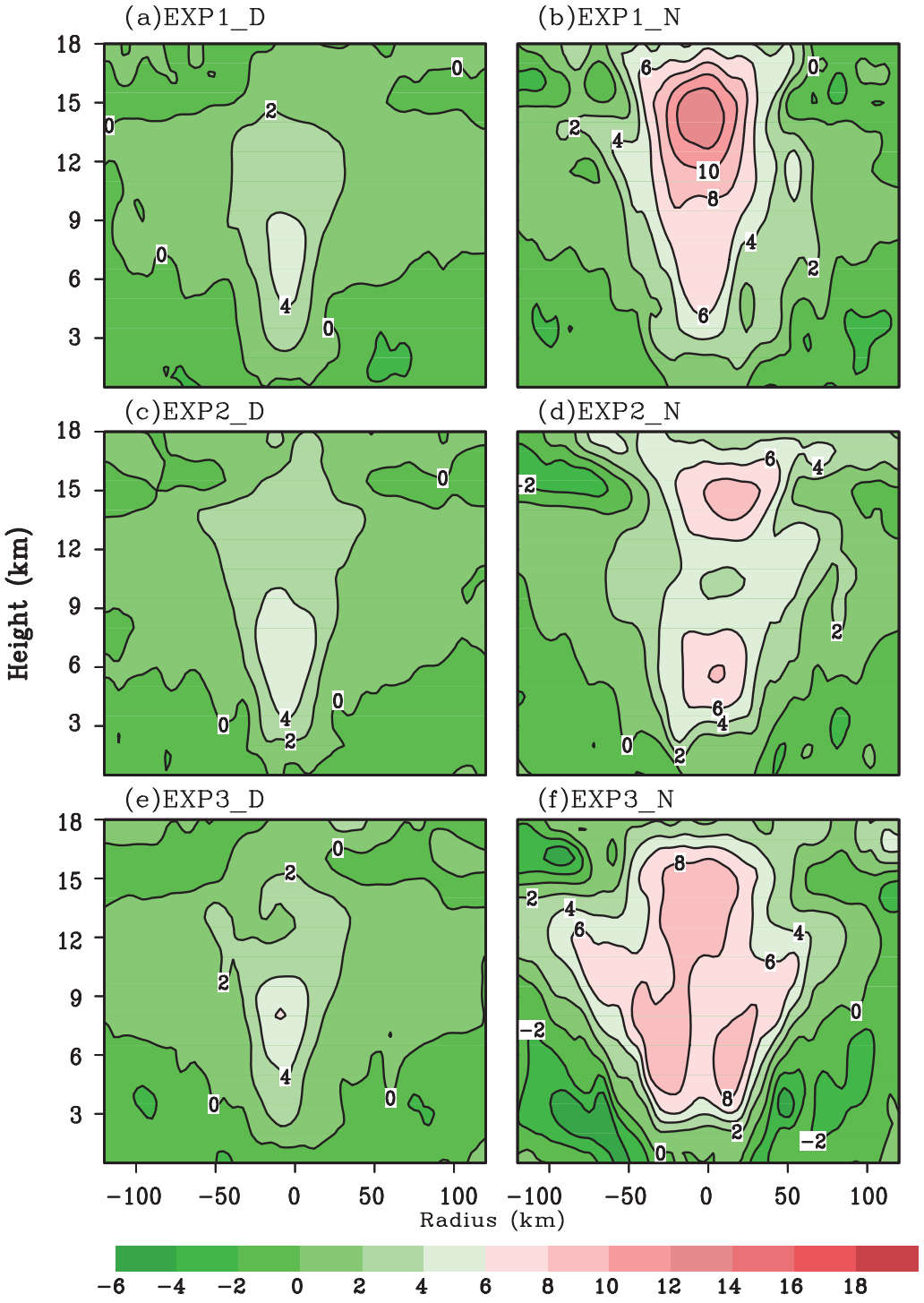

Fig. 10. Horizontal–vertical cross sections of the temperature perturbations (units: K) in the sensitivity experiments at $t = 96$ h: (a) EXP1_D; (b) EXP1_N; (c) EXP2_D; (d) EXP2_N; (e) EXP3_D; (f) EXP3_N. For an explanation of the different experiment types, see the text (section 4). The x-axis represents the east-west cross section across the TC center (units: km).

secondary circulations, resulting in a large variability of TC warm-core structure. By this reasoning, the conclusion here may represent the scenario for TCs with different intensity and structure. For instance, under favorable environmental conditions, strong CBs likely favor a stronger TC and thus a preferred upper-level warm core. In contrast, weak convective activity in the TC inner-core area may lead to a much lower entity. Moreover, in the current model configuration, TCs develop under the most favorable environmental conditions (i.e., no mean flows). In reality, a TC is also highly dependent on the underlying oceanic state, the large-scale environment, and storm-scale dynamics (Wu et al., 2011; Ge et

al., 2013; Liang et al., 2014). Hence, more sensitivity experiments involving complex environmental flows should be conducted in the future.

Acknowledgements. This work was jointly sponsored by the National Key Basic Research Program of China (Grant No. 2015CB452803), the National Natural Science Foundation of China (Grant No. 41275095), the "Six peaks of high-level talent" funding project of Jiangsu, the Key University Science Research Project of Jiangsu Province (Grant No. 14KJA170005), and the China Meteorological Administration Henan Key Laboratory of Agrometeorological Support and Applied Technique (Grant No. AMF201403). This paper is Earth system modeling center (ESMC) contribution number 032.

REFERENCES

Braun, S. A., 2002: A cloud-resolving simulation of Hurricane Bob (1991): Storm structure and eyewall buoyancy. *Mon. Wea. Rev.*, **130**, 1573–1592.

Chen, H., and D.-L. Zhang, 2013: On the rapid intensification of Hurricane Wilma (2005). Part II: Convective bursts and the upper-level warm core. *J. Atmos. Sci.*, **70**, 146–172.

Dai, A. G., 2001: Global precipitation and thunderstorm frequencies. Part II: Diurnal variations. *J. Climate*, **14**, 1112–1128.

Durden, S. L., 2013: Observed tropical cyclone eye thermal anomaly profiles extending above 300 hPa. *Mon. Wea. Rev.*, **141**, 4256–4268.

Emanuel, K. A., 1986: An air-sea interaction theory for tropical cyclones. Part I: Steady-state maintenance. *J. Atmos. Sci.*, **43**, 585–604.

Ge, X., Y. Ma, S.W. Zhou, and T. Li, 2014: Impacts of the diurnal cycle of radiation on tropical cyclone intensification and structure. *Adv. Atmos. Sci.*, **31**, 1377–1385, doi: 10.1007/s00376-014-4060-0.

Ge, X. Y., T. Li, and M. Peng, 2013: Effects of vertical shears and mid-level dry air on tropical cyclone developments. *J. Atmos. Sci.*, **70**, 3859–3875.

Hack, J. J., and W. H. Schubert, 1986: Nonlinear response of atmospheric vortices to heating by organized cumulus convection. *J. Atmos. Sci.*, **43**, 1559–1573.

Halverson, J. B., J. Simpson, G. Heymsfield, H. Pierce, T. Hock, and L. Ritchie, 2006: Warm core structure of Hurricane Erin diagnosed from high altitude dropsondes during CAMEX-4. *J. Atmos. Sci.*, **63**, 309–324.

Hawkins, H. F., and D. T. Rubsam, 1968: Hurricane Hilda, 1964. II: Structure and budgets of the hurricane on October 1, 1964. *Mon. Wea. Rev.*, **96**, 617–636.

Hawkins, H. F., and S. M. Imbembo, 1976: The structure of a small, intense hurricane—Inez 1966. *Mon. Wea. Rev.*, **104**, 418–442.

Hendricks, E. A., and M. T. Montgomery, 2004: The role of "vortical" hot towers in the formation of tropical cyclone Diana (1984). *J. Atmos. Sci.*, **61**, 1209–1232.

Heymsfield, G. M., J. B. Halverson, J. Simpson, L. Tian, and T. P. Bui, 2001: ER-2 Doppler radar investigations of the eyewall of Hurricane Bonnie during the Convection and Moisture Experiment-3. *J. Appl. Meteor.*, **40**, 1310–1330.

Holland, G. J., 1997: The maximum potential intensity of tropical cyclones. *J. Atmos. Sci.*, **54**, 2519–2541.

Holland, G. J., T. D. Keenan, and G. D. Crane, 1984: Observations of a phenomenal temperature perturbation in Tropical Cyclone Kerry (1979). *Mon. Wea. Rev.*, **112**, 1074–1082.

Hong, S.-Y., and J.-O. J. Lim, 2006: The WRF single-moment 6-class microphysics scheme (WSM6). *Journal of the Korean Meteorological Society*, **42**, 129–151.

Hong, S.-Y, Y. Noh, and J. Dudhia, 2006: A new vertical diffusion package with an explicit treatment of entrainment processes. *Mon. Wea. Rev.*, **134**, 2318–2341.

Knaff, J. A., S. A. Seseske, M. DeMaria, and J. L. Demuth, 2004: On the influences of vertical wind shear on symmetric tropical cyclone structure derived from AMSU. *Mon. Wea. Rev.*, **132**, 2503–2510.

Liang, J., L. G. Wu, and H. J. Zhong, 2014: Idealized numerical simulations of tropical cyclone formation associated with monsoon gyres. *Adv. Atmos. Sci*., **31**, 305–315, doi: 10.1007/s00376-013-2282-1.

Lin, Y. L., R. D. Rarley, and H. D. Orville, 1983: Bulk parameterization of the snow field in a cloud model. *J. Appl. Meteor.*, **22**, 1065–1092.

Mlawer, E. J., S. J. Taubman, P. D. Brown, M. J. Iacono, and S. A. Clough, 1997: Radiative transfer for inhomogeneous atmospheres: RRTM, a validated correlated-k model for the longwave. *J. Geophys. Res.*, **102**, 16 663–16 682.

Melhauser, C., and F. Q. Zhang, 2014: Diurnal radiation cycle impact on the pregenesis environment of Hurricane Karl (2010). *J. Atmos. Sci.*, **71**, 1241–1259.

Mellor, G. L., and T. Yamada, 1982: Development of a turbulence closure model for geophysical fluid problems. *Rev. Geophys. Space Phys.*, **20**, 851–875.

Nesbitt, S. W., and E. J. Zipser, 2003: The diurnal cycle of rainfall and convective intensity according to three years of TRMM measurements. *J. Climate*, **16**, 1456–1475.

Nolan, D. S., Y. Moon, and D. P. Stern, 2007: Tropical cyclone intensification from asymmetric convection: Energetics and efficiency. *J. Atmos. Sci.*, **64**, 3377–3405.

Ohno, T., and M. Satoh, 2014: On the Warm core of the tropical cyclone formed near the tropopause. *J. Atmos. Sci.*, doi: 10.1175/JAS-D-14-0078.1. (in press)

Powell, M. D., E. W. Uhlhorn, and J. D. Kepert, 2009: Estimating maximum surface winds from hurricane reconnaissance measurements. *Wea. Forecasting*, **24**, 868–883.

Schubert, W. H., and J. J. Hack, 1982: Inertial stability and tropical cyclone development. *J. Atmos. Sci.*, **39**, 1687–1697.

Stern, D. P., and D. S. Nolan, 2012: On the height of the warm core in tropical cyclones. *J. Atmos. Sci.*, **69**, 1657–1680.

Tao, W. K., S. Lang, J. Simpson, C. H. Sui, B. Ferrier, and M. D., Chou, 1996: Mechanisms of cloud-radiation interaction in the Tropics and midlatitudes. *J. Atmos. Sci.*, **53**, 2624–2651.

Webster, P. J., and G. L. Stephens, 1980: Tropical upper-tropospheric extended clouds: Inferences from winter MONEX. *J. Atmos. Sci.*, **37**, 1521–154.

Willoughby, H. E., 1990: Gradient balance in tropical cyclones. *J. Atmos. Sci.*, **47**, 265–274.

Wu, L. G., J. Liang, and C.-C. Wu, 2011: Monsoonal influence on Typhoon Morakot (2009). Part I: Observational analysis. *J. Atmos. Sci.*, **68**, 2208–2221.